ISSN: 2688-8645

Study of Multifactorial Effects on Well Wall Stability Based on Finite Element Modeling

Hongyong Guo, Zhiyu Zhou, Bingyue Han

College of Petroleum Engineering. Xi'an Shiyou University, Xi'an, Shaanxi 710065, China

Abstract

Drilling is a key link in oil and gas field development, and well wall stability is crucial to the success rate of drilling works and subsequent production.introducing the shear fracture trend (Ts) as an evaluation index, the effects of different geostress differentials, wellbore pressure,, and laminar structure on the stability of the well wall are investigated. The study shows that: as the ground stress difference decreases, the wellbore rupture risk decreases significantly, and the rupture pattern changes from a specific direction to a more uniform distribution; the minimum value of Ts increases when the internal pressure of the wellbore increases, and the damage tendency is weakened at a specific azimuthal angle in particular; when there is a laminar structure, rupture is prone to occur in the location of laminar structures, but the increase of the laminar In the presence of laminar structures, the laminar location is prone to rupture, but increasing the laminar spacing does not expand the damage range, but rather intensifies the damage on the laminar surfaces.

Keywords

Well Wall Stability; Linear Elastic Modelling; Shear Damage Trends; Layer Structure.

1. Introduction

With the development of the global economy and the increase in energy demand, exploration and exploitation activities for oil and gas resources have become more frequent. Drilling engineering, as a critical component of oil and gas field development, not only affects the efficiency and cost of development but also directly relates to operational safety and environmental protection. In this process, wellbore stability is a key technical challenge that determines the success or failure of drilling projects and the smooth operation of subsequent oil and gas production.

The study of wellbore stability began in 1940 when Westergaard[1] published works on the analysis methods of rock mechanics parameters related to wellbore stability, marking the start of pure mechanical studies on wellbore stability. Early research assumed that formation rocks were entirely homogeneous, disregarded the effects of drilling fluid column pressure, and presumed equal horizontal and vertical stresses to quantitatively investigate the stress field around the wellbore, leading to mathematical descriptions of elastic-plastic stress distributions around straight wells. Biot[2] introduced the theory of poroelasticity in 1955, which was further developed by Bowen and Lubinski[3] to explain rock constitutive relationships. Hubbert[4] and Willis first applied Kirsch's elastic solution to predict the stability of vertical wellbores under far-field stress and constant wellbore fluid pressure; Fairhurst[5], based on linear elastic theory, mathematically described the stress distribution around the wellbore at various well deviation angles considering the inclination between formations or boreholes. Bradley[6] established a wellbore stability model capable of predicting wellbore collapse and hydraulic fracturing-induced fracture losses, summarizing the impact of well deviation angles

ISSN: 2688-8645

and azimuths on wellbore stability, although these models mostly assumed rocks as linearly elastic materials without considering fluid flow effects.

As time progressed, research into wellbore stability became increasingly sophisticated, incorporating more complex factors. VM.Maury and J.M.Sauzay[7] summarized the factors affecting wellbore stability, including stress distribution around the wellbore, differences in horizontal stresses, rock deformation characteristics, and additional stresses caused by drilling fluid column pressure and temperature. Santarelli[8] and Brown[9] included stress-related elastic moduli in borehole stability analysis, using generalized Hooke's law to describe stress-strain relationships, finding that maximum tangential stress often concentrated within the surrounding rock rather than at the wellbore wall. Aadnoy[10] and Chenevert[11] proposed a semi-analytical model that considered the effect of rock anisotropy on inclined borehole stability; Ong[12] and Roegiers[13] improved this model, adopting anisotropic shear failure criteria and expressing stress as a function of borehole radius. Li et al[14]. developed a borehole stability analysis software named Bore-3D based on this work, widely used in the oil and gas industry. Gupta and Zaman (1994) pointed out that since most rock layers are not completely isotropic, anisotropic models provide a more accurate representation of reality.

Early studies on wellbore stability primarily relied on isotropic linear elasticity assumptions, attributing wellbore collapse to shear failure due to stresses exceeding rock strength, eventually forming a stable elliptical shape with "cat ear" features[15]. The Mohr-Coulomb failure criterion has been an essential tool for identifying where failures occur in brittle formations, and many scholars have utilized information from borehole collapse shapes to invert in-situ stresses and make real-time predictions[16]. Recently, Liu Yu et al[17]. (2022) established a new wellbore stability model for multi-weak-plane shale formations, analyzing the influence of weak plane groups, weak plane orientation, shale strength degradation, and collapse cycles on wellbore instability. Based on the aforementioned research, this paper adopts a linear elastic model combined with shear slip trend calculations to predict the stability of the surrounding rock around the wellbore and conducts sensitivity analysis on relevant parameters to explore the key factors influencing wellbore stability.

2. Methodology

From the perspectives of statics, geometry, and physics, the mathematical-physical equations corresponding to linear elastic steady-state problems are derived as follows:

Balance equation:

$$\frac{\partial \sigma_{xx}}{\partial x}+\frac{\partial \sigma_{xy}}{\partial y}+\frac{\partial \sigma_{xz}}{\partial z}+f_x=0 \tag{1}$$

$$\frac{\partial \sigma_{xy}}{\partial x}+\frac{\partial \sigma_{yy}}{\partial y}+\frac{\partial \sigma_{yz}}{\partial z}+f_y=0 \tag{2}$$

$$\frac{\partial \sigma_{xz}}{\partial x}+\frac{\partial \sigma_{yz}}{\partial y}+\frac{\partial \sigma_{zz}}{\partial z}+f_z=0 \tag{3}$$

Geometric equations:

$$\varepsilon_{xx}=\frac{\partial u}{\partial x} \quad \varepsilon_{xz}=\frac{\partial w}{\partial y}+\frac{\partial v}{\partial z} \tag{4}$$

$$\varepsilon_{yy}=\frac{\partial v}{\partial y} \quad \varepsilon_{yz}=\frac{\partial w}{\partial x}+\frac{\partial v}{\partial z} \tag{5}$$

$$\varepsilon_{zz}=\frac{\partial w}{\partial z} \quad \varepsilon_{xy}=\frac{\partial u}{\partial y}+\frac{\partial v}{\partial x} \tag{6}$$

ISSN: 2688-8645

Constitutive equation:

$$\begin{pmatrix}\sigma_{xx}\\ \sigma_{yy}\\ \sigma_{zz}\\ \sigma_{xz}\\ \sigma_{yz}\\ \sigma_{zz}\end{pmatrix}=\frac{E}{(1+\nu)(1-2\nu)}\begin{pmatrix}1-\nu & \nu & \nu & & & \\ \nu & 1-\nu & \nu & & & \\ \nu & \nu & 1-\nu & & & \\ & & & 0.5-\nu & & \\ & & & & 0.5-\nu & \\ & & & & & 0.5-\nu\end{pmatrix}\begin{pmatrix}\varepsilon_{xx}\\ \varepsilon_{yy}\\ \varepsilon_{zz}\\ \varepsilon_{xz}\\ \varepsilon_{yz}\\ \varepsilon_{xy}\end{pmatrix} \tag{7}$$

Here, σ_{xx}, σ_{yy}, and σ_{zz} denote the principal stresses in the three directions of the rectangular coordinate system; ε_{xx}, ε_{yy}, and ε_{zz} denote the corresponding principal strains; σ_{xy}, σ_{xz}, and σ_{yz} denote the shear stresses in the three directions; ε_{xy}, ε_{xz}, and ε_{yz} denote the corresponding shear strains; *u*, *v*, and *w* denote the displacements in the three directions of the rectangular coordinate system; E denotes Young's modulus; and ν denotes Poisson's ratio.

3. Well Wall Surrounding Rock Stability Analysis

3.1. Shear Trends in the Well Wall

When the shear stress acting upon a fault plane exceeds the resistance to sliding, it may be anticipated that the rock will undergo frictional sliding along the fault plane. This mechanical behaviour adheres to what is termed Coulomb's criterion. Coulomb's criterion describes the relationship governing the minimum shear stress required for rock to slide along a fault plane.

$$\tau = S_0 + \mu\sigma_n \tag{8}$$

In the equation, τ denotes the shear stress along the fracture plane, S_0 is termed cohesion (the strength of pre-existing defects arising from healing mechanisms), μ represents a material property known as the coefficient of static friction, and σ_n signifies the effective normal stress. The shear stress and normal stress acting on a fault plane are functions of the fault's orientation relative to the horizontal plane and can be expressed as:

$$\cos(2\beta) = -\frac{\sigma_1 - \sigma_3 - 2S_0}{\sigma_1 + \sigma_3 + 2S_0}(\sigma_1 > \sigma_3 > 0) \tag{9}$$

$$\sigma_{n(\beta)} = \frac{1}{2}(\sigma_1 + \sigma_3) + \frac{1}{2}(\sigma_1 - \sigma_3)\cos 2\beta \tag{10}$$

$$\tau_{(\beta)} = \frac{1}{2}(\sigma_1 - \sigma_3)\sin 2\beta \tag{11}$$

In the formula, β denotes the angle between the normal direction of the fault plane and the first principal direction, σ_1 represents the maximum principal stress, and σ_3 signifies the minimum principal stress.

The shear tendency (Ts) of a plane oriented at angle b to the first principal stress in any direction is defined as:

$$T_s = \frac{\tau_{(\beta)} - S_0}{\sigma_{n(\beta)}} \tag{12}$$

ISSN: 2688-8645

Ts represents the shear stress trend. By calculating this trend, we can predict the stability of the wellbore and potential geological risks. When the value exceeds 1, there is a risk of wellbore failure.

3.2. The Effect of Differential Ground Stress on Borehole Wall Stability

Differential stress significantly influences borehole wall stability. Reviewing relevant literature indicates that the difference between maximum and minimum horizontal in-situ stresses typically fluctuates between 0 and 20 megapascals (MPa). Given this range, this section will investigate the effect of differential stress on borehole wall stability by varying the maximum horizontal stress. To conduct this study, five operational scenarios were established, as shown in Table 1.

Table 1. Geotechnical Properties of Rock and Soil Layers under Different Operating Conditions

Operating Condition	Maximum horizontal stress	Minimum horizontal stress	Wellbore pressure	Young's modulus	Poisson ratio
Operating Condition 1	10MPa	10MPa	1MPa	45GPa	0.3
Operating Condition 2	15MPa	10MPa	1MPa	45GPa	0.3
Operating Condition 3	20MPa	10MPa	1MPa	45GPa	0.3
Operating Condition 4	25MPa	10MPa	1MPa	45GPa	0.3
Operating Condition 5	30MPa	10MPa	1MPa	45GPa	0.3

It is noteworthy that when the local stress difference reached 20 MPa, the stress distribution along the wellbore exhibited significant fluctuations, with peak stress values occurring particularly at positions approximately 90°, 180° and 270° around the wellbore. Conversely, when the local stress difference was 0 MPa, the stress distribution along the wellbore remained relatively stable, showing no pronounced localised stress concentration phenomena.

As illustrated in Fig 1, the distribution cloud diagram depicts the shear tendency along the borehole wall under varying in-situ stress differentials. From left to right and top to bottom, the conditions correspond to in-situ stress differentials of 0 MPa, 5 MPa, 10 MPa, 15 MPa, and 20 MPa respectively. It can be observed that as the in-situ stress differential increases, the shear trend exhibits an overall upward trajectory. The maximum shear trend values are successively 2.135, 2.635, 2.997, 3.262, and 3.466. This indicates that as the in-situ stress differential grows, the risk of wellbore fracture also increases.

Further examination of these contour plots reveals that as the in-situ stress differential increases, the spatial distribution of shear trends along the wellbore exhibits significant alterations. Horizontally, shear tendencies diminish, whereas vertically and at specific angles around the wellbore—namely 45°, 135°, 225°, and 315°—shear tendencies markedly intensify. This trend indicates that under conditions of substantial in-situ stress differentials, the risk of fracture within the wellbore is heightened in these specific directions.

Overall, these cloud images provide crucial insights into wellbore stability, particularly where significant stress differentials exist. By comparing these visualisations, we gain a deeper understanding of how stress differentials influence shear tendencies within the wellbore and the resulting fracture risks. These findings offer valuable guidance for optimising wellbore design and construction strategies, thereby enhancing the safety and reliability of the wellbore.

ISSN: 2688-8645

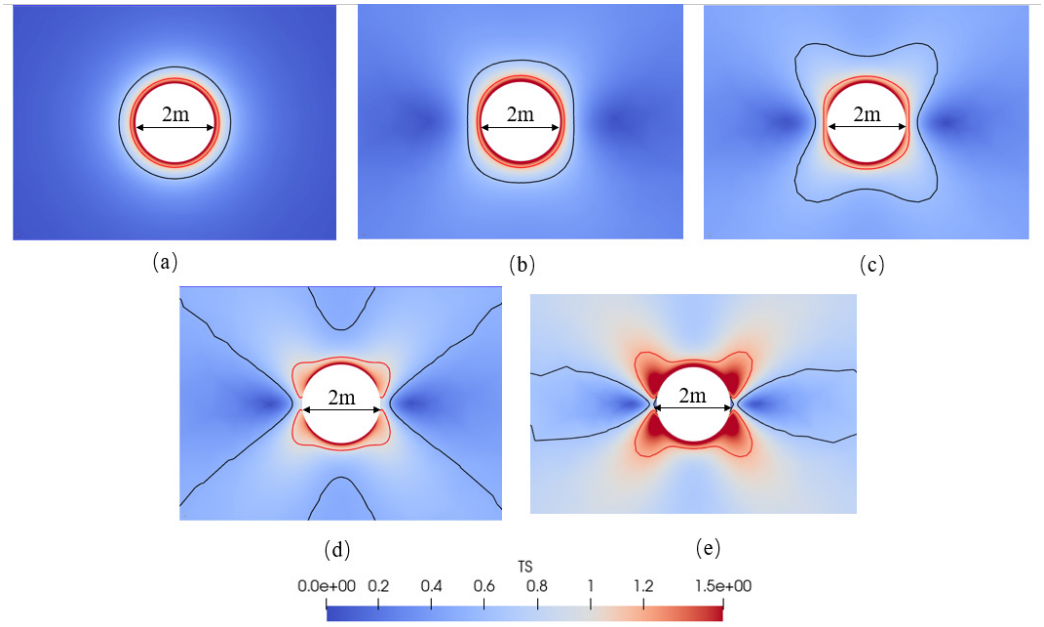

Fig 1. Contour plot of wellbore shear stress distribution, with red representing Ts values of 1 and black representing Ts values of 0.5:(a) Ground stress difference 0 MPa; (b) Ground stress difference 5 MPa; (c) Ground stress difference 10 MPa; (d) Ground stress difference 15 MPa; (e) Ground stress difference 20 MPa.

3.3. The Effect of Different Borehole Pressure on Wellbore Stability

The pressure within the borehole significantly influences the stability of the borehole wall. Given this scope, this section will investigate the impact on borehole wall stability by altering the borehole pressure. To conduct this study, the borehole pressure is set to a series of distinct values as shown in Table 2, namely 0 MPa, 1 MPa, 2 MPa, 3 MPa, and 4 MPa, whilst maintaining the maximum horizontal stress and minimum horizontal stress constant. Subsequently, we shall investigate the stress distribution on the borehole wall based on these established borehole pressures.

Table 2. Geotechnical Properties of Rock and Soil Layers under Different Operating Conditions

Operating Condition	Maximum horizontal stress	Minimum horizontal stress	Wellbore pressure	Young's modulus	Poisson ratio
Operating Condition 1	20MPa	10MPa	0MPa	45GPa	0.3
Operating Condition 2	20MPa	10MPa	1MPa	45GPa	0.3
Operating Condition 3	20MPa	10MPa	2MPa	45GPa	0.3
Operating Condition 4	20MPa	10MPa	3MPa	45GPa	0.3
Operating Condition 5	20MPa	10MPa	4MPa	45GPa	0.3

As shown in Fig 2, the distribution cloud diagram illustrates the shear trend distribution of the wellbore wall under different wellbore pressure conditions. From left to right and top to bottom, the conditions correspond to wellbore pressures of 0 MPa, 1 MPa, 2 MPa, 3 MPa, and 4 MPa respectively. It is observed that the shear trend generally decreases with increasing borehole pressure, yielding maximum shear trend values of 8.69571, 2.366, 1.64955, 1.28532, and

ISSN: 2688-8645

1.13647 respectively. This indicates that the risk of borehole wall failure progressively diminishes as borehole pressure increases.

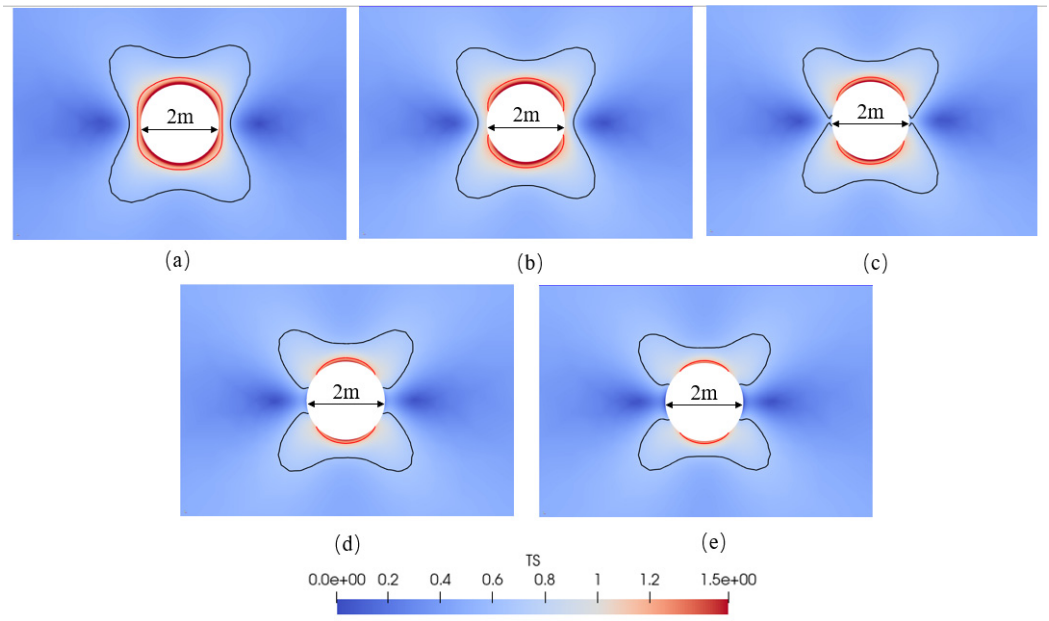

Fig 2. Contour plot of wellbore shear stress distribution, with red representing Ts values of 1 and black representing Ts values of 0.5:(a) Borehole pressure 0 MPa; (b) Borehole pressure 1 MPa; (c) Borehole pressure 2 MPa; (d) Borehole pressure 3 MPa; (e) Borehole pressure 4 MPa;

Further analysis of these contour plots reveals that borehole wall stability improves with increasing borehole pressure. Specifically, as borehole pressure rises, shear trends diminish across all directions, indicating enhanced resistance to wall failure. This trend holds positive implications for borehole wall design and construction, as higher borehole pressures correlate with reduced fracture risk, thereby improving wall safety performance.

In summary, these cloud images provide crucial insights into wellbore stability, particularly under varying wellbore pressure conditions. By comparing these visualisations, we gain a more comprehensive understanding of how wellbore pressure influences shear tendencies within the wellbore walls and the consequent fracture risk. This data holds significant reference value for optimising wellbore design and construction strategies, thereby contributing to ensuring the reliability and safety of the wellbore structure.

3.4. Effect of Different Layer Spacing on Well Wall Stability

Stratigraphic surface spacing is the vertical distance between two neighbouring stratigraphic surfaces. It is affected by a number of factors such as depositional environment, sediment grain size and depositional rate. In fine-grained sediments (e.g., shale), the lamination surface spacing may be small, while in rocks formed by coarse-grained sediments (e.g., sandstone), the lamination surface spacing is relatively large. Therefore, this section investigates the effect of laminations on well wall stability by varying different lamination spacings.

As shown in Fig 3, Fig 3(a) is a schematic diagram of the location of the laminae, in which the white area represents the laminae and the blue area indicates the geotechnical part. In order to deeply study the influence of the layer spacing on the stability of the well wall, we refer to the relevant literature and set up four groups of different working conditions, as shown in

Table **3**, which are 0.2 m, 0.4 m, 0.6 m and 0.8 m. The working conditions are 0.2 m, 0.4 m, 0.6 m and 0.8 m respectively. By analysing the well wall stability under different formation spacing, we aim to explore the influence of the variation of formation spacing on the well wall stability.

ISSN: 2688-8645

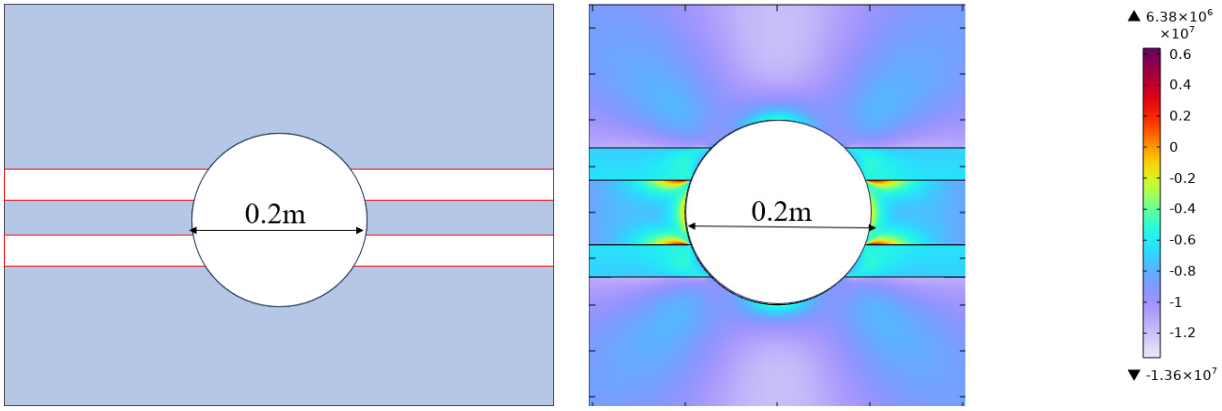

(a) (b)

Fig 3. Simplified Well Wall Layering Schematic and Stress Distribution Cloud Map:(a)Schematic location of the laminations (b) Stress distribution cloud map

Table 3. Layer spacing and its nature under different working conditions

working condition	interval between layers	Young's modulus of laminae	laminar Poisson's ratio	Young's modulus for geotechnical formations	Poisson's ratio for rock and soil layers
Condition 1	0.2m	5GPa	0.22	45GPa	0.3
Condition 2	0.4m	5GPa	0.22	45GPa	0.3
Condition 3	0.6m	5GPa	0.22	45GPa	0.3
Condition 4	0.8m	5GPa	0.22	45GPa	0.3

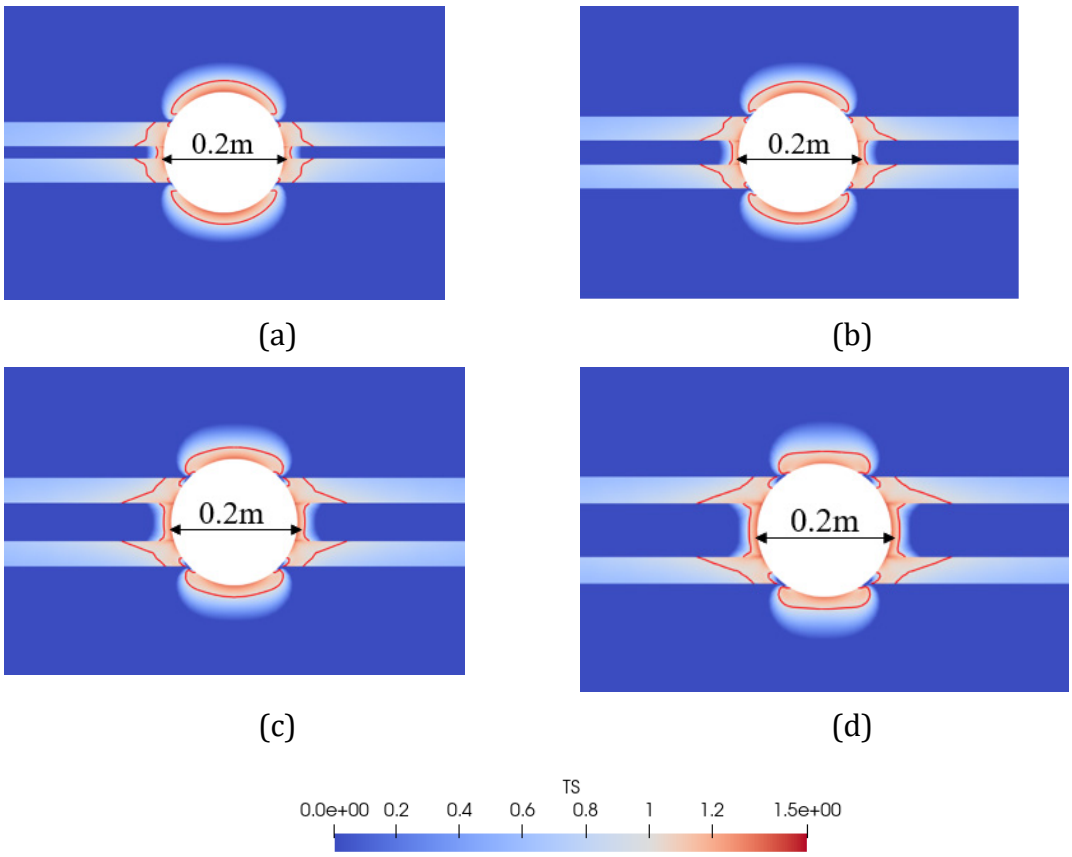

(a) (b)

(c) (d)

Fig 4. Contours of the distribution of shear trend of the well wall under different laminae spacing, red represents Ts value of 1:(a) Layer spacing 0.2 m; (b) Layer spacing 0.4 m; (c) Layer spacing 0.6 m; (d) Layer spacing 0.8 m

ISSN: 2688-8645

As shown in Fig 4, this is a schematic diagram of the shear damage trend of the well wall with different spacing of the laminae. By comparing the four different sets of cloud diagrams, it can be found that the damage range in the middle of the laminae does not increase with the increase of laminae spacing, but the damage range on the laminae surface increases with the increase of spacing. Analysing the reason, the increase of the ply spacing makes the stress distribution on the ply surface more concentrated. Larger ply spacing means that the distance between adjacent ply surfaces increases, and the stress is distributed more unevenly in these areas, resulting in higher local stresses on the ply surfaces, which are more prone to damage.

3.5. Effect of Different Layer Properties on Well Wall Stability

The nature of different interstratification can also have an impact on well wall stability. Based on this, this section sets up different gradient of laminations to study their influence on well wall stability. As shown in Fig 5, Fig 5(a) shows a schematic diagram of the location of the laminae, in which the white area represents the laminae, the blue area indicates the geotechnical part, and the laminae area is divided into four regions from top to bottom.

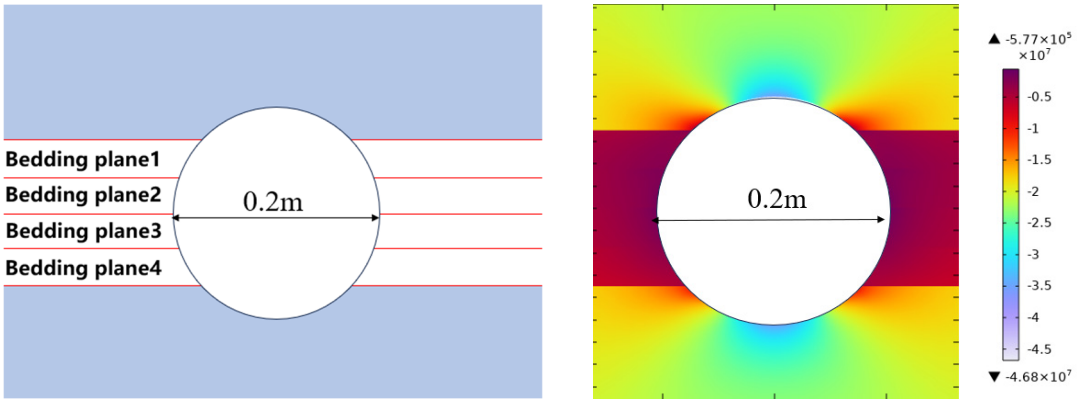

(a) (b)

Fig 5. Simplified well wall stratigraphy schematic and stress distribution cloud diagram:(a) Schematic location of the laminations (b) Stress distribution cloud map

Through reviewing relevant literature, this study sets 4 groups of different gradient of laminated elastic modulus in order from top to bottom, and the specific settings are shown in Table **4**. Through these 4 groups of different gradient of laminated elastic modulus settings, this study aims at exploring the influence of different laminated properties on the stability of the well wall.

Table 4. Nature of stratification zones under different working conditions

working condition	Young's modulus of laminated region 1	Young's modulus of laminated region 2	Young's modulus of laminated region 3	Young's modulus of laminated region 4	Young's modulus for geotechnical formations
Condition 1	5GPa	6GPa	7GPa	8GPa	45GPa
Condition 2	5GPa	7.5GPa	10GPa	12.5GPa	45GPa
Condition 3	5GPa	10GPa	15GPa	20GPa	45GPa
Condition 4	5GPa	15GPa	25GPa	35GPa	45GPa

As shown in Fig 6, this is a schematic diagram of the shear trend of the well wall under different elastic modulus gradient layer properties. The following patterns can be found through comparison: (1) the damage range of the layer above and the upper layer is basically the same, which indicates that the nature of the layer in these areas has less influence on the damage

ISSN: 2688-8645

range; (2) the damage range of the part of the geotechnical layer below the layer decreases gradually with the increase of the gradient of the elastic modulus of the layer. This suggests that higher modulus of elasticity of the laminae can effectively reduce the damage extent of the geotechnical layer below, probably because the laminae with high modulus of elasticity can better disperse and transfer the stresses, thus protecting the geotechnical layer below (3) the laminae in region 1, because of the larger gap between Young's modulus and the geotechnical layer, the rupture extent is even greater, and the harder laminae under the 'Region 1' The stiffer structure of the laminae underneath helps to mitigate this effect and reduces the risk of further downward transmission of damage.

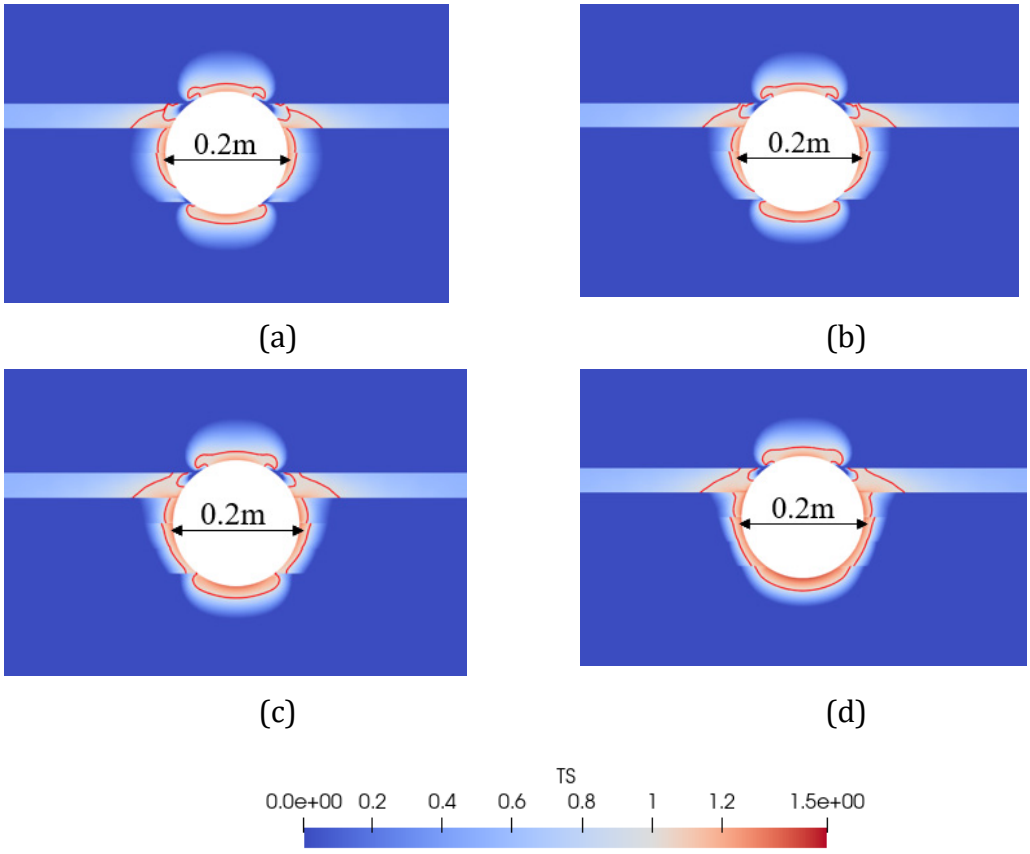

Fig 6. Cloud contours of well wall shear trend distribution under different laminae properties, red represents Ts value of 1:(a) Laminated elastic modulus gradient 5GPa-6GPa-7GPa-8GPa (b) Laminated elastic modulus gradient 5GPa-7.5GPa-10GPa-12.5GPa; (c) Laminated elastic modulus gradient 5GPa-10GPa-15GPa-20GPa; (d)Laminated elastic modulus gradient 5GPa-15GPa-25GPa- 35GPa.

4. Conclusion

Drilling constitutes a pivotal stage in oil and gas field development, with wellbore stability posing a significant technical challenge throughout. This issue not only impacts drilling success rates but also determines the smooth progression of subsequent oil and gas production. Consequently, this paper introduces the shear failure trend (Ts) as an indicator for assessing failure conditions around the wellbore. When Ts falls below 1, it signifies potential failure risk. This approach involves constructing a numerical solution model and validating its accuracy through analytical solutions.

(1) By examining shear failure trends near the wellbore under four distinct formation stress differentials (20 MPa, 15 MPa, 10 MPa, and 5 MPa), it was observed that the risk of wellbore

fracture decreases significantly as the formation stress differential diminishes. Under larger stress differentials, the wellbore tends to develop 'cat's ear' fracture patterns oriented along the direction of minimum horizontal principal stress, as well as at 45°, 135°, 225°, and 315° angles. As the local stress differential diminishes, this fracture pattern gradually transforms into a more uniformly distributed ring around the wellbore.

(2) As borehole pressure increased from 1 MPa to 7 MPa, the minimum value of Ts progressively rose, indicating enhanced overall borehole stability. Notably, the failure zone along the minimum horizontal principal stress direction markedly diminished with increasing borehole pressure, demonstrating strengthened resistance to fracture development.

(3) In the presence of a laminated structure, the location of the laminae is the place where rupture is more likely to occur, regardless of the angle of the laminae. Increasing the spacing of the laminae does not lead to an increase in the extent of damage in the interlaminar region, but it does increase the extent of damage on the laminar surface because it increases the local stress concentration. For the rock portion below the laminae, the extent of damage in this region decreases instead as the gradient of the elastic modulus of the laminae increases.

References

[1] WESTERGAARD H M. Plastic state of stress around a deep well [M]. Harvard University, 1939.

[2] BIOT M A. Theory of elasticity and consolidation for a porous anisotropic solid [J]. Journal of applied physics, 1955, 26(2): 182-185.

[3] LUBINSKI A. The theory of elasticity for porous bodies displaying a strong pore structure; proceedings of the Proc, F, 1954 [C].

[4] HUBBERT M K, WILLIS D G. Mechanics of hydraulic fracturing [J]. Transactions of the AIME, 1957, 210(01): 153-168.

[5] FAIRHURST C. Measurement of in-situ rock stresses. With particular reference to hydraulic fracturing [J]. Rock Mech;(United States), 1964, 42-47.

[6] BRADLEY, W. B. Failure of Inclined Boreholes [J]. Journal of Energy Resources Technology, 1979, 101(4): 232.

[7] MAURY V. Rock failure mechanisms identification: A key for wellbore stability and reservoir behaviour problem [J]. SPE/ISRM Rock Mechanics in Petroleum Engineering, 1994, SPE-28049-MS.

[8] SANTARELLI F J. Theoretical and experimental investigation of the stability of the axisymmetric wellbore [J]. Imperial College London, 1987.

[9] SANTARELLI F J, BROWN E T. Performance of Deep Well Bores In Rock With a Confining Pressure-dependent Elastic Modulus [J]. International Society for Rock Mechanics, 1987.

[10] AADNOY B S. Modeling of the Stability of Highly Inclined Boreholes in Anisotropic Rock Formations (includes associated papers 19213 and 19886) [J]. SPE Drilling Engineering, 1988, 3(3): 259-268.

[11] AADNOY B S, CHENEVERT M E. Stability of highly inclined boreholes [J]. SPE Drilling Engineering, 1987, 2(364-374).

[12] ONG S H, ROEGIERS J C. Horizontal Wellbore Collapse in an Anisotropic Formation; proceedings of the Spe Production Operations Symposium, F].

[13] ROEGIERS J C. Lecture: Stability And Failure of Circular Openings [J]. 1989.

[14] LI X, ROEGIERS J, TAN C. Collaborative Development of a Wellbore Stability Analysis Software With Determination of Horizontal Stress Bounds From Well Bore Data [J]. 1996.

[15] D., I., GOUGH, et al. Stress orientations from borehole wall fractures with examples from Colorado, east Texas, and northern Canada [J]. Can J Earth Sci, 1982, 19(7): 1358-1370.

[16] GUANGQUAN L, YI W, JUNHAI C. Analysis of the Maximum Horizontal Principal Stress Based onWellbore Collapse Information [J]. Petroleum Drilling Techniques, 2012, 40(1): 5.

[17] LIU Y. Study on wellbore stability of shaleformation with multi weak plane [D]; Northeast Petroleum University, 2022.